

The Contribution of the Non-axisymmetrical Component in Inner Core to the Maximum Intensity of the Simulated Tropical Cyclones

Satoki Tsujino and Kazuhisa Tsuboki

Hydrospheric Atmospheric Research Center, Nagoya University, Nagoya, Japan



1. Introduction

The theoretical Tropical Cyclone (TC) models having two-dimensional axisymmetric structure present the structure and intensity of real TCs very well (e.g. Emanuel's MPI theory; Emanuel, 1986). However, two-dimensional axisymmetric models do not include non-axisymmetric structure in TC. Wang (2002a,b) indicated that non-axisymmetry in an idealized TC influences the intensity and structure of TC, using a three-dimensional model. This suggests that a three-dimensional model is necessary to predict more accurate maximum intensity of TC. In addition, we believe that non-axisymmetric effects should be included in axisymmetric theoretical models.

The present study uses a three-dimensional non-hydrostatic model named the Cloud Resolving Storm Simulator (CRSS) to estimate quantitatively how non-axisymmetry influences TC maximum intensity (i.e. maximum wind speed in quasi-steady state) by analyzing angular momentum budget in the inner core region. Since we investigate the relationship of maximum intensity to non-axisymmetric component, we analyze angular momentum budgets for TCs which have different maximum intensities. Moreover, we analyze the energetics of maintaining mechanism of non-axisymmetric components by energy budget.

2. Experimental Configurations

In this study, we used the CRSS model, which is a three-dimensional non-hydrostatic model (Tsuboki and Sakakibara, 2007).

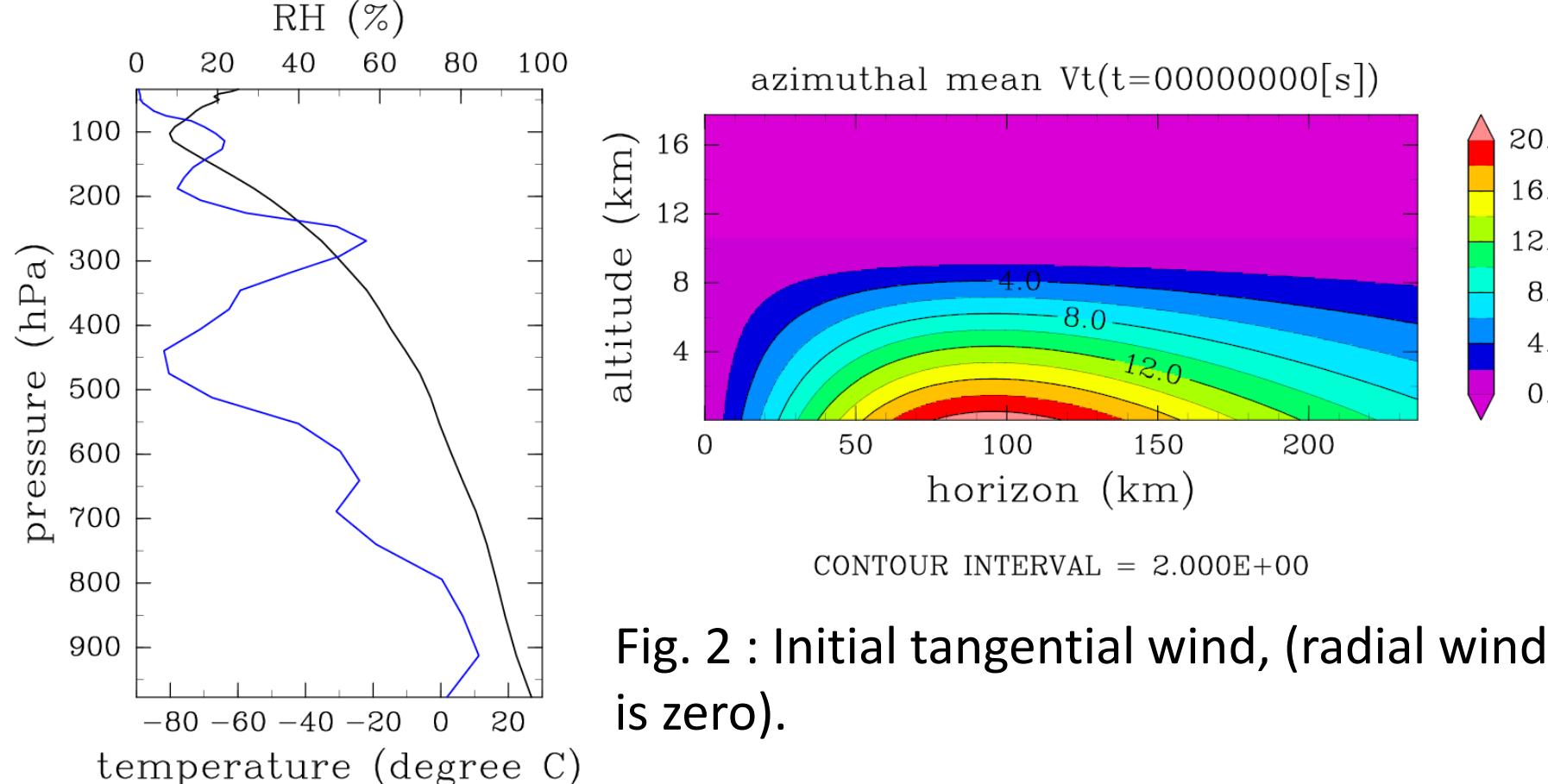


Fig. 1 : Vertical profile of initial temperature (Black) and vapor (Blue) horizontally constant.

For the purpose of this study, we conducted four parameter sweep experiments. According to Bryan and Rotunno (2009), the maximum wind speed of TC is sensitive to the process of the exchange of heat and momentum in the sea surface.

So, we swept the parameters of CE (coefficient of heat exchange) and CD (coefficient of momentum exchange) as table 2.

Table 2 : In four experiments, CE and CD value. "1.0", "1.5" are multiplication factors for CE, CD.

Experiment	CTL	CE1.5CD1.5	CE1.5	CD1.5
CE	1.0	1.5	1.5	1.0
CD	1.0	1.5	1.0	1.5

Table 1 : Configuration of Experiments.

Horizontal Grid	4 km x 4 km
Calculating Domain	2000 km x 2000 km
Vertical Grid	40 layers (domain top : 23 km)
Initial Data	Temperature and Vapor: A Sounding Data in Western North Pacific Ocean (Fig.1). Wind: $V(r,z) = \frac{z_0 - z}{z_0} \frac{40 \times (r/r_0)}{1 + (r/r_0)^3}$, ($z \leq 10 \text{ km}$) $Z_0 = 10 \text{ km}$, $r_0 = 120 \text{ km}$ (Fig.2).
SST	303 K
Integral Time	250 hour
Surface Process	Bulk aerodynamic formulation
Lateral Boundary	Open boundary
Coriolis Parameter	15 degree N (f-plane)

Bulk aerodynamic formulation :

$$\begin{aligned} \tau &= -\rho_a |V_a| C_D V_a, \\ F_{qv} &= -\rho_a |V_a| C_E (q_{va} - q_{vs}), \\ F_\theta &= -\rho_a |V_a| C_E (\theta_a - \theta_s). \end{aligned}$$

3. Result

All experiments reached quasi-steady state by 250 hour (Fig.3).

In this study, we defined the period from 240 hour to 250 hour as quasi-steady state, and used data that time to analyze budgets.

In this period, we observed remarkable Non-axisymmetric structure (Fig. 4).

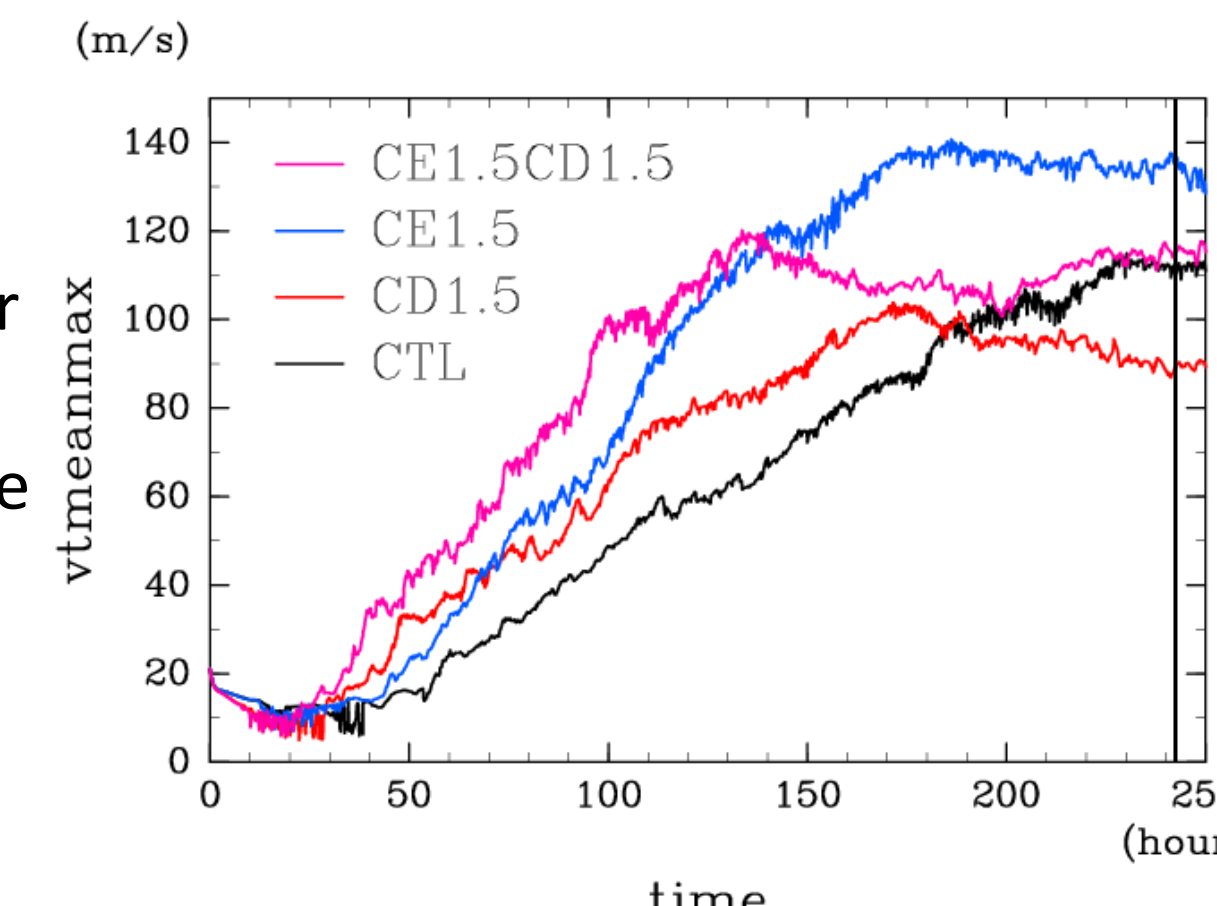


Fig. 3 : Time series of tangential wind (azimuthally averaged) of experiments. Quasi-steady state : 240 - 250 hour.

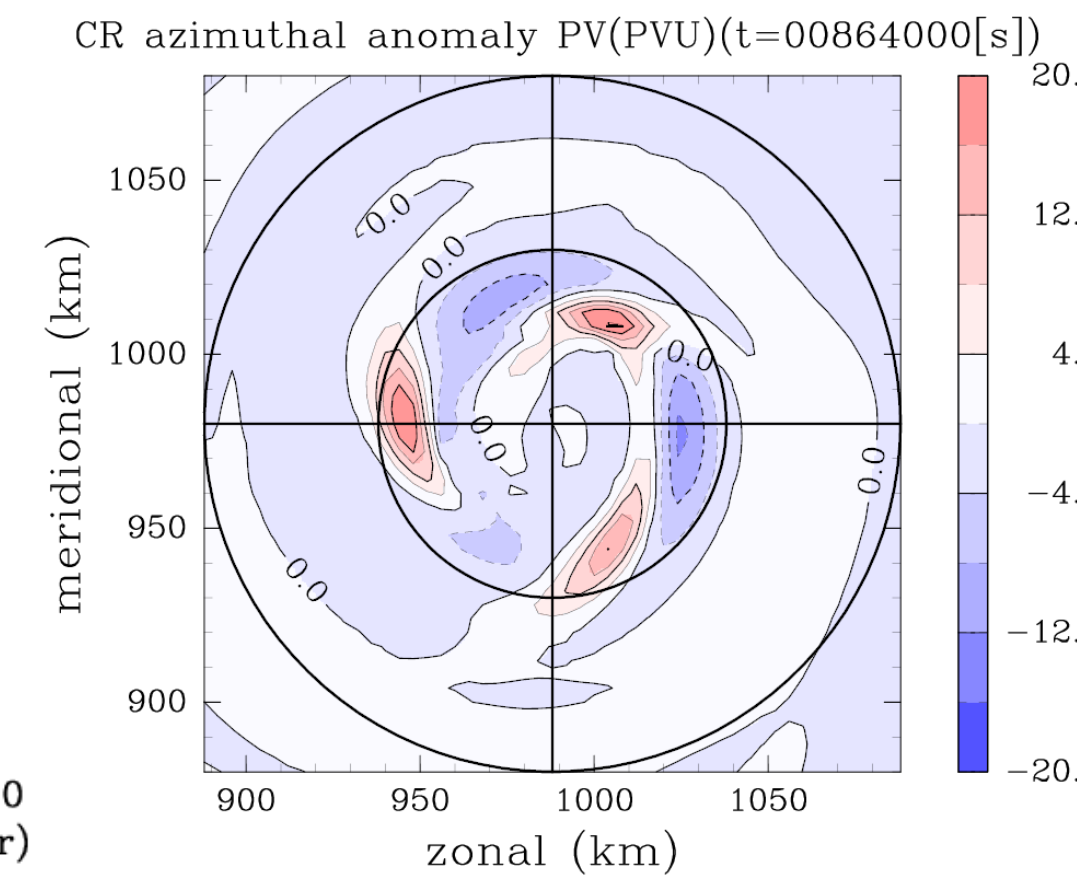


Fig. 4 : Azimuthal anomaly of PV at 1.2 km height. (time = 240 hour, unit = PVU)

4. 1. Angular Momentum Budgets

$$\phi(r, \theta, z, t) = \underbrace{\bar{\phi}(r, z, t)}_{\text{Axisymmetric component}} + \underbrace{\phi'(r, \theta, z, t)}_{\text{Non-axisymmetric component}}$$

$$\bar{\phi}(r, z, t) = \frac{1}{2\pi} \int_0^{2\pi} \phi(r, \theta, z, t) d\theta$$

Equation of angular momentum budget :

$$\frac{\partial}{\partial t} (r\bar{v}) = \underbrace{\left(-\left(\frac{1}{r} \frac{\partial}{\partial r} (r^2 \bar{u}\bar{v}) + \frac{1}{\rho_0} \frac{\partial}{\partial z} (r\rho_0 \bar{w}\bar{v}) \right) - fr\bar{u} \right)}_{\text{FLXM}} + r\text{Turb.v}$$

$$\underbrace{\left(-\left(\frac{1}{r} \frac{\partial}{\partial r} (r^2 \bar{u}'\bar{v}') + \frac{1}{\rho_0} \frac{\partial}{\partial z} (r\rho_0 \bar{w}'\bar{v}') \right) \right)}_{\text{FLXE}}$$

① FLXM : The acceleration of tangential wind due to axisymmetric component.

② Turb. : Turbulence and surface friction.

③ FLXE : The acceleration of tangential wind due to non-axisymmetric component.

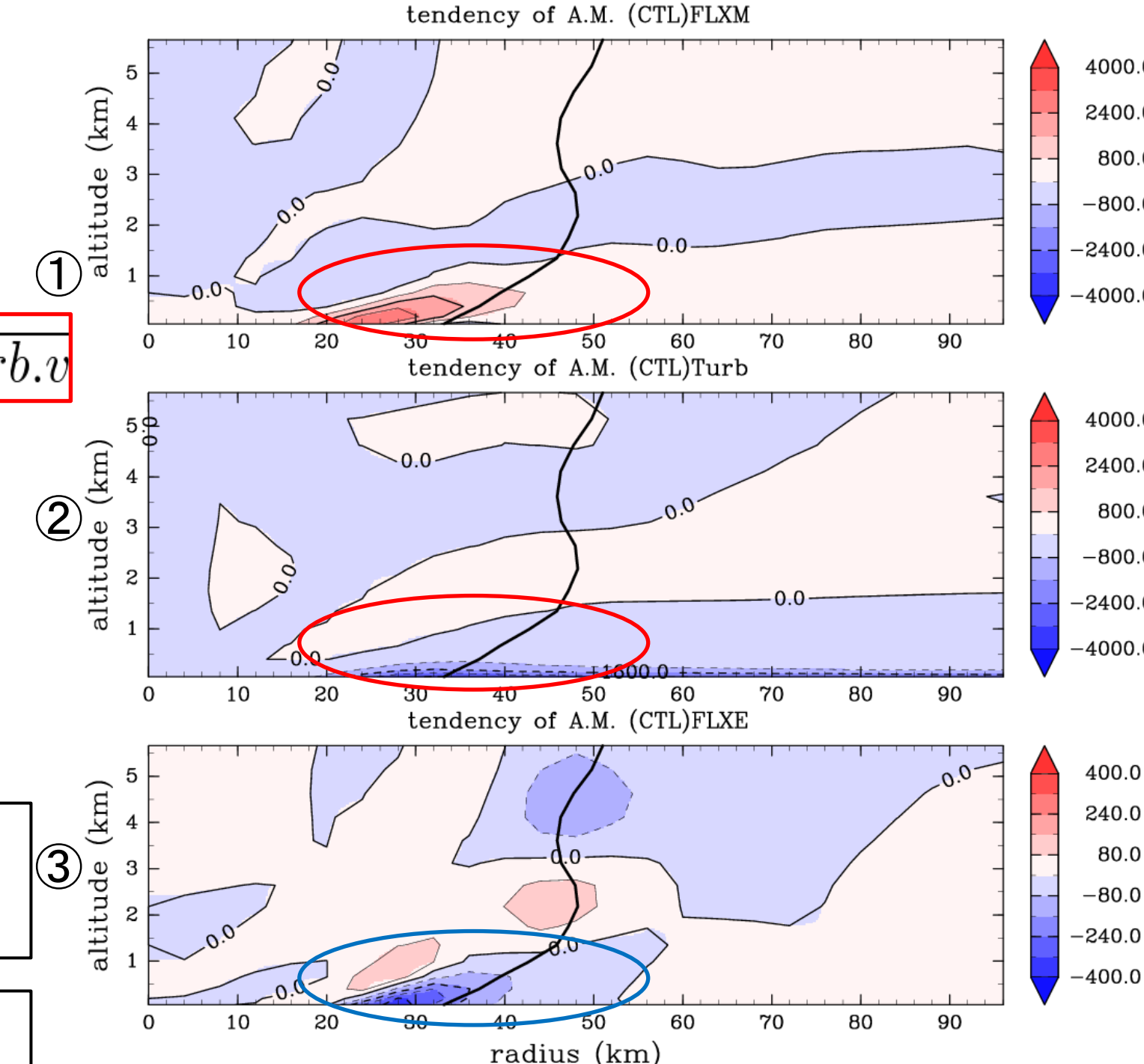


Fig. 5 : Contributions of term ①, ②, ③. (unit = m²/s²) Positive value is acceleration of axisymmetric wind. Note that this results are time average over 240 - 250 hour.

Experiment	CTL	CE1.5CD1.5	CE1.5	CD1.5
Maximum wind speed (m/s)	111	115	134	89
Max FLXM (m ² /s ²)	3227	2633	4942	1789
Min FLXE (m ² /s ²)	-386	-350	-693	-141
FLXE/FLXM (%)	12.0	13.2	14.0	7.9

Table 3 : For four experiments, the relationship of the maximum wind speed to the contribution (i.e. |FLXE/FLXM|) of non-axisymmetric component in the inner core region, which radial distance is less than 100 km and height is below 4 km. Max FLXE is maximum FLXM in the inner core, Min FLXE is minimum FLXE in the inner core.

4. 2. Kinetic Energy Budgets

Equation of Kinetic Energy budget (Non-axisymmetric component) :

$$\begin{aligned} \frac{\partial \bar{K}'}{\partial t} &= - \left(\frac{1}{r} \frac{\partial (r\bar{u}'\bar{K}')}{\partial r} + \frac{1}{\rho_0} \frac{\partial (\rho_0 \bar{w}'\bar{K}')}{\partial z} \right) \\ &\text{①} - \left(\frac{1}{r} \frac{\partial (r\bar{u}'\bar{K}')}{\partial r} + \frac{1}{\rho_0} \frac{\partial (\rho_0 \bar{w}'\bar{K}')}{\partial z} \right) \\ &\text{②} - \left\{ \frac{\partial \bar{u}}{\partial r} \bar{u}' + \bar{u}' \frac{\partial \bar{v}}{\partial r} + \bar{u}' \frac{\partial \bar{v}'}{\partial r} - \bar{v}' \frac{\partial \bar{u}'}{\partial r} \right\} \\ &\text{③} - \left\{ \bar{w}' \frac{\partial \bar{u}}{\partial z} + \bar{w}' \frac{\partial \bar{v}}{\partial z} \right\} \\ &\text{④} - \frac{1}{\rho_0} \left\{ \frac{1}{r} \frac{\partial (r\bar{u}'\bar{p}')}{\partial r} + \bar{p}' \frac{\partial \bar{w}'}{\partial z} + \frac{d}{dz} (\ln \rho_0) \bar{p}' \bar{w}' \right\} \\ &\text{⑤} + \bar{v}' \cdot \text{Turb} \bar{v}' \\ &\text{⑥} \end{aligned}$$

① Flux divergence of kinetic energy by axisymmetric flow

② Flux divergence of kinetic energy by non-axisymmetric flow

Sinks for tendency of kinetic energy.

③ Conversion from axisymmetric flow to non-axisymmetric flow by barotropic process

④ Conversion from axisymmetric flow to non-axisymmetric flow by baroclinic process

⑤ Conversion from potential energy to kinetic energy

Sources for tendency of kinetic energy.

⑥ Diffusion by turbulence and surface friction (Not show).

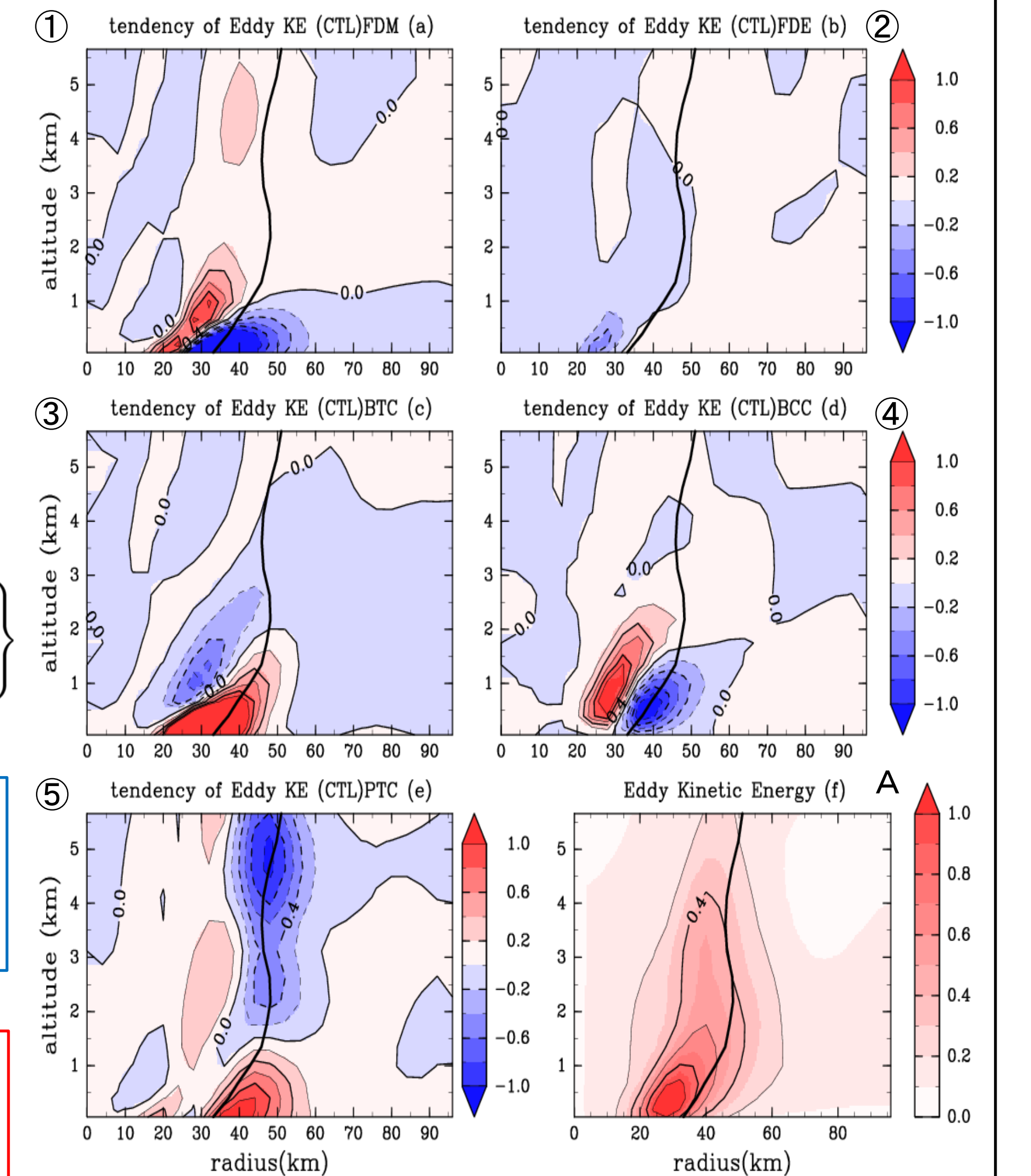


Fig. 6 : Contributions of term ①, ②, ③, ④, ⑤ and profile of kinetic energy (A) for CTL. Positive value is source for kinetic energy. Note that this results are time average over 240 - 250 hour. Unit is m²/s³ (① - ⑤), x 100 m²/s² (A).

5. Conclusion

The present study showed that non-axisymmetric components have negative contributions for the maximum intensity (i.e. deceleration for the maximum wind velocity) in the inner core. In addition, we showed that this deceleration due to non-axisymmetric components is about 10% of the acceleration due to axisymmetric components and the deceleration increases with the maximum wind velocity.

Therefore, we infer that non-axisymmetric components should be considered for prediction by the MPI theory for intense TCs. This result suggests that the effect of non-axisymmetric components should be considered in theoretical models of the maximum potential intensity.

Moreover, we performed energy budget analysis of non-axisymmetric components. This showed that energy of non-axisymmetric components is supplied with conversion of potential energy of non-axisymmetric component to kinetic energy, conversion by barotropic process and conversion by baroclinic processes.